

Low Loss Ultra-Small Branches in a Silicon Photonic Wire Waveguide

Atsushi SAKAI[†], Tatsuhiko FUKAZAWA[†], *Nonmembers*,
and Toshihiko BABA^{†a)}, *Regular Member*

SUMMARY We theoretically and experimentally demonstrate low loss branches in a Si photonic wire waveguide. Approximate calculation by the two-dimensional finite-difference time-domain (2-D FDTD) method and detailed design by the 3-D FDTD method indicate that low excess loss less than 0.2 dB is expected for a μm -size bend-waveguide-type branch at a wavelength of $1.55 \mu\text{m}$. This branch is fabricated in a silicon-on-insulator substrate and the loss is evaluated to be 0.3 dB. This value is small enough to construct a very compact branching circuit.

key words: *integrated optics, optical waveguide, branch circuit, SOI, FDTD*

1. Introduction

For a dense wavelength division multiplexing system with several hundred channels, the size reduction and high-density integration of optical circuits such as wavelength multi/demultiplexers and cross connect switches are crucial. The most fundamental issue is to miniaturize optical waveguides. However, conventional silica-based waveguides have small flexibility in optical wirings because of large bends and branches, each occupying $\text{mm}^2\text{-cm}^2$ area. To realize a compact optical circuit of mm^2 in total area, the bend radius must be of μm order. The photonic crystal waveguide [1] is one of the candidates that clear this issue, so it is attracting much attention. However, it requires a complex design theory and a fine fabrication process. Another simpler solution is an ultra-high Δ waveguide, where Δ is the relative refractive index difference defined as $(n_1^2 - n_2^2)/2n_1^2$ for core index n_1 and cladding index n_2 .

A commercially available silicon-on-insulator (SOI) substrate is usable for such a high- Δ waveguide. The Si slab ($n_1 \sim 3.5$) is used as a core and the SiO_2 ($n_2 \sim 1.45$) layer is used as a cladding in the transparent wavelength range of $\lambda = 1.3\text{--}1.55 \mu\text{m}$. Therefore, Δ of this waveguide is as large as 45%. Of course, this wafer is used for electronic circuits. Thus, the SOI substrate can be a platform of functional opto-electronic circuits. So far, rib-type waveguides in an SOI substrate have been demonstrated with a low propagation loss less than 0.5 dB/cm [2], [3]. However, the bend radius was of mm order because of the weak optical

confinement. For μm order bends, Si layer must be the completely etched down to be the rectangular shape, as shown in Fig. 1.

Such rectangular waveguide has also been reported [4]. However, only the propagation loss of the straight waveguide was discussed, and other components such as bends and branches have not been investigated yet. In a previous work, we fabricated this type of waveguide, which satisfies the singlemode condition, and showed that 1) the propagation loss is $\sim 10 \text{ dB/mm}$ at $\lambda = 1.55 \mu\text{m}$ and it is dominated by the scattering loss caused by the high- Δ , 2) the group index is larger than the material index, and 3) the bend loss can be less than 1 dB, when the bend radius is only $1 \mu\text{m}$ [5]. Based on these results, we designed and fabricated ultra-small branches in an SOI substrate, and demonstrated the low excess loss in this work. We first estimated the excess loss in several branches by the 2-dimensional (2-D) finite-difference time-domain (FDTD) method [6]. For two structures showing low loss in this calculation, we designed the structural detail by the 3-D FDTD method. Then, we fabricated a bend-waveguide-type branch, the best structure for low excess loss, and evaluated its characteristics.

2. 2-D FDTD Analysis of Various Branches

The FDTD method is very powerful for simulating electromagnetic properties in arbitrary structure with a high index contrast. In a 3-D FDTD calculation, however, a large computer memory and a long CPU time are required. The 2-D FDTD method with the equivalent index approximation significantly reduces the load

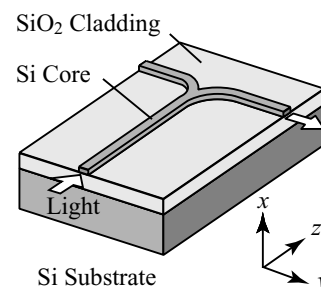


Fig. 1 Schematic of Si rectangular channel photonic wire waveguide and the coordinate system.

Manuscript received October 9, 2001.

[†]The authors are with Division of Electrical and Computer Engineering, Yokohama National University, Yokohama-shi, 240-8501 Japan.

a) E-mail: baba@dnj.ynu.ac.jp

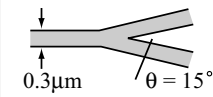
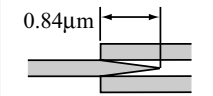
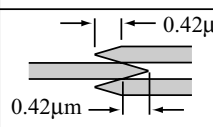
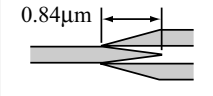
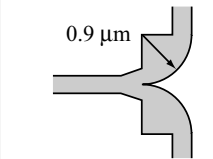
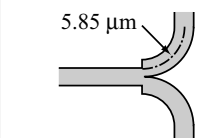
of calculation and gives a rough but reasonable estimation. In all calculations of this paper, wavelength λ is fixed to $1.55\ \mu\text{m}$. In this section, the polarization is fixed to that having the electric field parallel to the yz plane and the magnetic field in the x direction. This corresponds to the transverse electric (TE)-like polarization in a 3-D channel which will be discussed in Sect.3. The equivalent index n_{eq} of the Si slab is assumed to be 2.6, and the channel width is $0.3\ \mu\text{m}$. Lateral claddings are air with an index of 1.0. They satisfy the singlemode condition at $\lambda = 1.55\ \mu\text{m}$. One side of the square Yee cell is $20\ \text{nm}$ ($\sim \lambda/30n_{\text{eq}}$). The time step is $0.04\ \text{fs}$, which satisfies Courant's stable condition. The magnetic field distribution of the analytically-derived guided mode is continuously excited around the channel. The excess loss of a branch is estimated from the ratio of total power from two waveguides beyond the branch ($P_{\text{out}} \equiv P_{\text{out1}} + P_{\text{out2}}$) to the input power observed near the excitation (P_{in}). Here, the excitation source locates $18\ \mu\text{m}$ from the branch. This is long enough to avoid that the reflected power from the branch is counted as the input power. To estimate P_{out} accurately, two waveguides beyond the branch are bent, so it looks like a T-branch, as illustrated in Fig.1. The analytical space is terminated by Mur's second-order absorbing boundary condition. Since the reflection at waveguide ends is not perfectly suppressed even with these boundaries, P_{out1} and P_{out2} are evaluated at points $16\ \mu\text{m}$ apart from the absorbing boundary. This is distant enough to estimate them before reflected waves reach these points.

Table 1 summarizes various branches modeled. The excess loss of simple Y branch (a) is estimated to be 2 dB when the branching angle is 15° . Although the excess loss may be reduced by a smaller angle, it makes the branch long, so it is not suitable for the purpose of this study. For modified antenna-coupled-type branches (b)–(d) [7], [8], the loss is less than 0.5 dB. Especially, (d) marks a minimum value of less than 0.1 dB. In branch (e), two fans with $0.9\text{-}\mu\text{m}$ -radius are connected to the input waveguide with a small taper. This structure is similar to a reported one [9], in which two corner mirrors are used at the branch. However, we rather employed the fans to avoid the unwanted reflection. The minimum loss is 0.3 dB, when guided modes are efficiently coupled to whispering gallery modes in each fan [10]. In branch (f), two bent waveguides are connected, so we call it bend-waveguide-type. When the bend radius is $5.85\ \mu\text{m}$, the loss is less than 0.1 dB.

3. Design by 3-D FDTD Method

For branches (d) and (f) showing $< 0.1\ \text{dB}$ loss in Sect.2, structural details are designed using the 3-D FDTD method. The thickness of Si and SiO_2 layers are assumed to be $0.32\ \mu\text{m}$ and $1.0\ \mu\text{m}$, respectively, to simulate the SOI wafer used in the experiment. The

Table 1 Various branch structures.

	Schematic	Loss
(a)		2.0 dB
(b)		0.5 dB
(c)		0.5 dB
(d)		< 0.1 dB
(e)		0.3 dB
(f)		< 0.1 dB

air above the Si core and Si substrate below the SiO_2 layer are also included in the analytical space. Indexes of Si, SiO_2 and air are assumed to be 3.45, 1.44 and 1.0, respectively. One side of the cubic Yee cell Δx is enlarged to $40\ \text{nm}$ ($\sim \lambda/11n_1$) to save the CPU time. The time step is $0.06\ \text{fs}$, which satisfies the Courant's stable condition. Although the polarization cannot be defined rigorously in a 3-D waveguide, the y component of the electric field is excited to simulate the TE-like mode. The waveguide width w is fixed to be $0.44\ \mu\text{m}$ ($= 11\Delta x$). This width satisfies the singlemode condition at $\lambda = 1.55\ \mu\text{m}$ and the peak of the electric field of the guided mode locates just at the center of the waveguide.

Figure 2 shows the x component of the magnetic field distribution in the antenna-coupled-type branch. Here, lengths l of the taper in both input and output waveguides are the same. For $l = 0.8\ \mu\text{m}$, the field exhibits the winding motion in the output waveguides. This motion is smaller for $l = 2.8\ \mu\text{m}$, but it still remains. This indicates that the rapid change of the structure at the branch excites radiation modes, which should be the excess loss, as shown in Fig. 3. The loss decreases monotonically with increasing l . However, it cannot be less than 1 dB. This result is different from that for the 2-D model shown in Table 1. We think that this difference comes from different zigzag paths

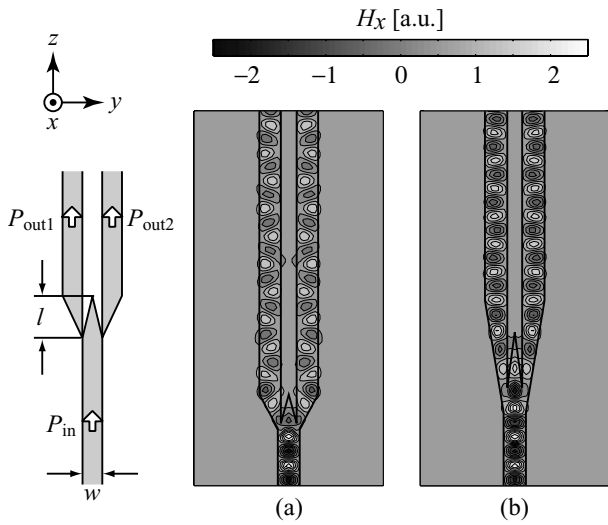


Fig. 2 Top view of the 3-D FDTD calculation model and the x component of magnetic field in antenna-coupled-type branches with $w = 0.44 \mu\text{m}$. (a) and (b) are for $l = 0.8 \mu\text{m}$ and $2.8 \mu\text{m}$, respectively.

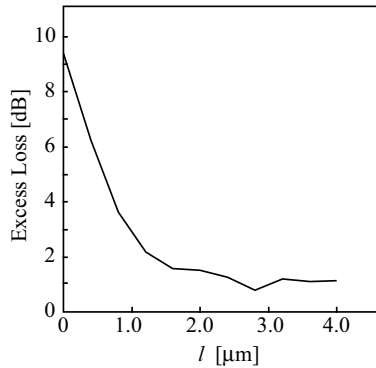


Fig. 3 Excess loss with taper length l in antenna coupled type with $w = 0.44 \mu\text{m}$, which is calculated by the 3-D FDTD method.

of light in the waveguide, which give different group indexes, i.e., 4–5 for 3-D model [5], while ~ 3 for the 2-D model. The different zigzag paths cause different excitations of multimodes at the branch and results in different optimum structures.

The x component of the magnetic field distribution in the bend-waveguide-type is shown in Fig. 4. The light is smoothly separated without any serious scattering at the branch and winding motion in output waveguides. The excess loss calculated with bend radius r is shown in Fig. 5. A similar 3-D calculation indicates that the bend loss is estimated to be 0.2–0.4 dB for radius assumed in Fig. 5. This figure shows the excess loss including the bend loss at the bend. It is estimated to be less than 0.4 dB for all radius assumed, and the minimum value is 0.20 dB for $r = 1.38 \mu\text{m}$.

We investigated the influence of asymmetry in the bend-waveguide-type. Figure 6 shows the change of the power branching ratio $P_{\text{out}1}/P_{\text{out}}$ calculated with

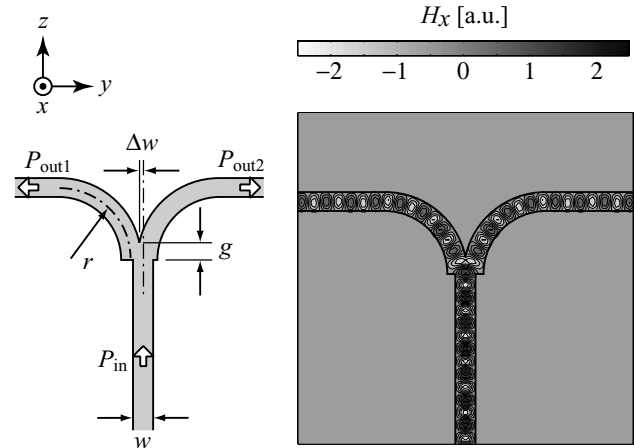


Fig. 4 Top view of the 3-D calculation model and the x component of magnetic field in bend-waveguide-type branch with $r = 1.78 \mu\text{m}$, $w = 0.44 \mu\text{m}$, $g = 0.28 \mu\text{m}$, and $\Delta w = 0 \mu\text{m}$.

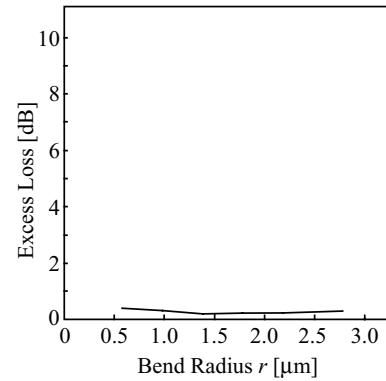


Fig. 5 Excess loss with bend radius r in bend-waveguide-type branch with $w = 0.44 \mu\text{m}$, which is calculated by 3-D FDTD method.

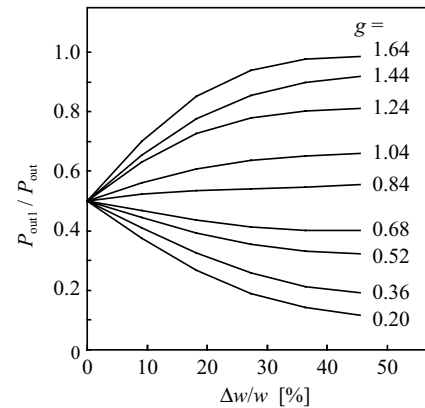


Fig. 6 Branching ratio with normalized shift $\Delta w/w$ of input waveguide for parameter g in bent-waveguide-type branch with $r = 2.18 \mu\text{m}$ and $w = 0.44 \mu\text{m}$.

the normalized shift $\Delta w/w$ of input waveguide measured from the center axis. The power branching ratio is strongly influenced by overlapping length g . For

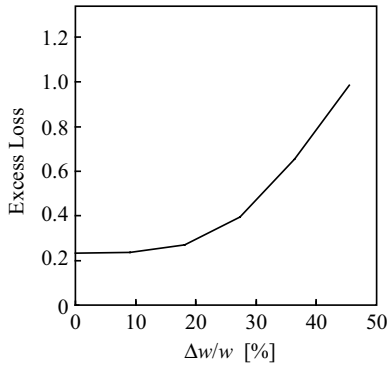


Fig. 7 Change of excess loss with $\Delta w/w$ in bend-waveguide-type branch with $r = 2.18 \mu\text{m}$, $w = 0.44 \mu\text{m}$ and $g = 0.32 \mu\text{m}$.

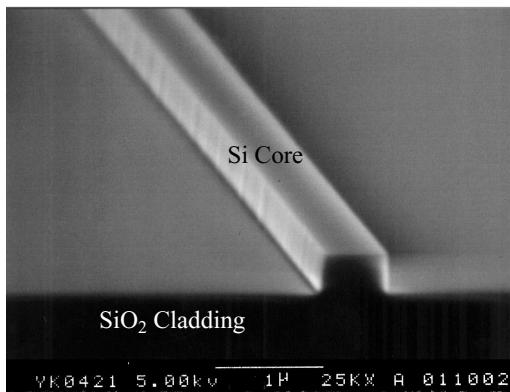


Fig. 8 SEM view of fabricated Si rectangular channel.

$g \leq 0.68 \mu\text{m}$, $P_{\text{out1}}/P_{\text{out}}$ decreases as $\Delta w/w$ increases. On the other hand, for $g \geq 0.84 \mu\text{m}$, it increases as $\Delta w/w$ increases. The critical point giving $P_{\text{out1}}/P_{\text{out}} = 0.5$ for any $\Delta w/w$ can be expected for $g \sim 0.80 \mu\text{m}$. The loss change with $\Delta w/w$ is shown in Fig. 7. It is relatively insensitive to $\Delta w/w$, e.g., the loss is still 0.3 dB for $\Delta w/w = 20\%$.

4. Fabrication and Measurement

We prepared a unibond-type SOI wafer (SOI TEC Inc.), which had a SiO_2 layer of $1.0\text{-}\mu\text{m}$ -thickness and a top p-type Si layer of $0.32 \mu\text{m}$ thickness. The fluctuation in the Si thickness was less than 20 nm inside a $7 \times 7 \text{mm}^2$ cleaved piece. The free carrier absorption loss is negligible compared with the scattering loss at rough sidewalls, since the resistivity of the Si layer is as high as $14 \Omega\text{cm}$. We used a field-emission-type electron beam (EB) lithography and CF_4 -based inductively coupled plasma (ICP) etching to fabricate the Si rectangular channel. After the EB-drawn pattern of the positive resist was transferred to a metal mask, the top Si layer was completely etched down by the ICP etching. Figure 8 is a scanning electron micrograph (SEM) of a cleaved end facet of the waveguide. Considering the retreat of the mask, the pattern width was designed to

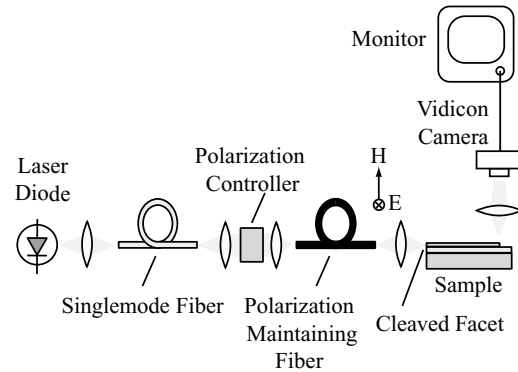


Fig. 9 Measurement setup of light propagation characteristics.

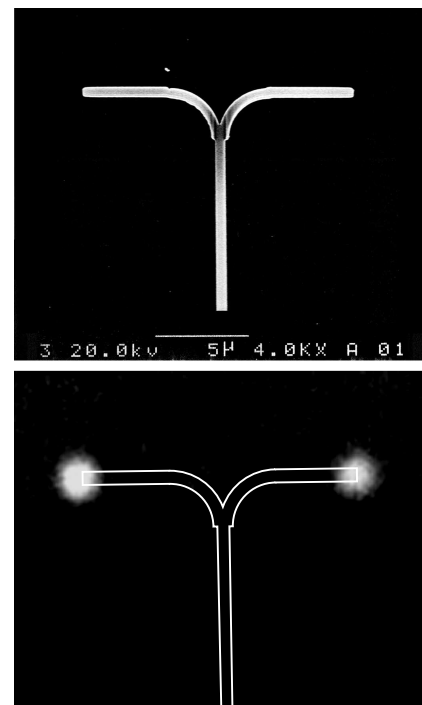


Fig. 10 Top view and NFP of light output for sample with $r = 2.75 \mu\text{m}$, $w = 0.47 \mu\text{m}$ and $g = 0.4 \mu\text{m}$.

be $0.5 \mu\text{m}$. The fabricated one is $0.47 \mu\text{m}$, which is close to the modeled value in Sect. 3. The sidewall angle of the waveguide is over 85° and the sidewall roughness is 20 nm in maximum value and 11 nm in deviation. For the Si layer in the unibond-type SOI wafer, the perfect crystal facet cannot be obtained by the cleavage. As shown in Fig. 8, however, the waveguide facet is smooth enough due to small cross sectional area.

The measurement setup is shown in Fig. 9. The light of $\lambda = 1.55 \mu\text{m}$ from a semiconductor laser is controlled to be TE-polarized and focused on the waveguide facet. The output end of the waveguide is terminated inside the wafer by the lithography and the etching. The light from this output end is detected by a vidicon camera from the top of the waveguide. Figure 10 shows the near field pattern (NFP) of the light

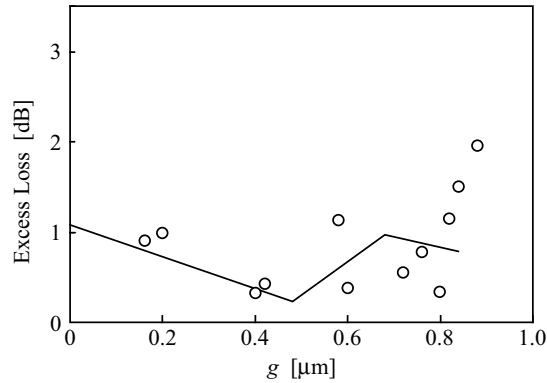


Fig. 11 Measured excess loss for $r = 2.75 \mu\text{m}$ (circle) and calculated results for $r = 2.78 \mu\text{m}$ (curves).

output from the bend-waveguide-type branch with $r = 2.75 \mu\text{m}$. As expected from the FDTD calculation, the light passes through the branch and is extracted from two output ends. Such NFP can be observed from the top without any irregular scattering at waveguide ends, since the mode size in the Si waveguide is smaller than the diffraction limit in air, and the radiation angle of the light output is over 180° [11]. This allows the evaluation of relative output power by the vidicon camera with the compensation of its nonlinearity. First, the waveguide loss was evaluated to be $\sim 10 \text{ dB/mm}$ by comparing output powers from different length straight waveguides. This value is almost the same as that evaluated previously by the Fabry-Perot resonance method [7]. Next, the excess loss at the branch was specified by comparing the output power from a simple bent waveguide and that from the branch, as shown in Fig. 11. Here, r is fixed to be $2.75 \mu\text{m}$ and the overlap length of two output waveguides g is changed. The loss takes the minimum value 0.3 dB for $g = 0.4 \mu\text{m}$. This result almost agrees with the 3-D FDTD calculation. The 0.3-dB -loss is small enough and difficult to explain its origin. One reason considered is the reflection at the input end of the branch. We expect a further low loss less than 0.1 dB by the slight modification of the input end.

Measured and calculated branching ratio are plotted with length g in Fig. 12. Nearly 60% data lie near $P_{\text{out}1}/P_{\text{out}} = 0.5$. Other data show larger values $0.7\text{--}0.8$. This is thought to be due to the complex dependence of the branching ratio on $\Delta w/w$ and g .

5. Conclusion

Ultra-small branches in a Si photonic wire waveguide were studied theoretically and experimentally. From the FDTD calculation, it was shown that the bend-waveguide-type branch achieved a low excess loss of 0.2 dB under the singlemode condition at $\lambda = 1.55 \mu\text{m}$. This branch was fabricated into an SOI wafer, and the excess loss was evaluated to be as low as 0.3 dB . This

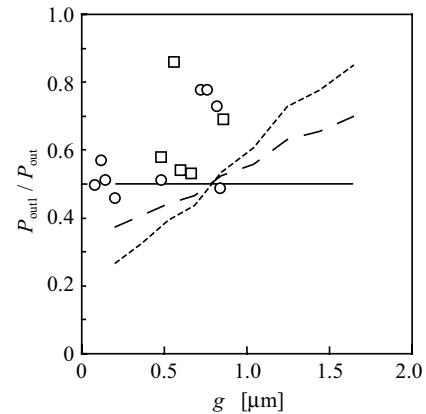


Fig. 12 Measured branching ratio for $\Delta w/w = 0\text{--}13\%$ (circle) and $16\text{--}22\%$ (square) with $r = 2.75 \mu\text{m}$. Calculated results for $\Delta w/w = 0\%$ (solid curve), 9% (dashed curve) and 18% (dotted curve) are also shown with $r = 2.78 \mu\text{m}$.

branch was constructed by $2.75\text{-}\mu\text{m}$ -radius bends, so the total area of the branch occupied only $(5 \mu\text{m})^2$ area. We can expect this waveguide and branch to drastically miniaturize some optical circuits such as H-tree branches.

Acknowledgement

We would like to thank Prof. Y. Kokubun, Prof. Y. Hirose and Associate Prof. H. Arai, Yokohama National University, and Prof. K. Iga and Prof. F. Koyama, Tokyo Institute of Technology, for valuable discussions.

References

- [1] T. Baba, N. Fukaya, and J. Yonekura, "Observation of light propagation in photonic crystal optical waveguides with bends," *Electron. Lett.*, vol.35, no.8, pp.654–655, April 1999.
- [2] J. Schmidtchen, A. Splett, B. Schuppert, and K. Petermann, "Low loss single mode optical waveguides with large cross-section in silicon-on-insulator," *Electron. Lett.*, vol.27, no.16, pp.1486–1488, Aug. 1991.
- [3] A.G. Rickman and G.T. Reed, "Silicon-on-insulator optical rib waveguides: Loss, mode characteristics, bends and y-junctions," *IEE Proc. Optoelectron.*, vol.141, no.6, pp.391–393, Dec. 1994.
- [4] K.K. Lee, D.R. Lim, H.-C. Luan, A. Agarwal, J. Foresi, and L.C. Kimerling, "Effect of size and roughness on light transmission in Si/SiO₂ waveguide: Experiments and model," *Appl. Phys. Lett.*, vol.77, no.11, pp.1617–1619, Sept. 2000.
- [5] A. Sakai, G. Hara, and T. Baba, "Propagation characteristics of ultrahigh-D optical waveguide on silicon-on-insulator substrate," *Jpn. J. Appl. Phys.*, vol.40, no.4B, pp.L383–L385, April 2001.
- [6] A. Taflov and S.C. Hagness, *Computational electrodynamics: the finite-difference time-domain method*, Second ed., Artech House Publishers, Boston, 2000.
- [7] M. Rangaraj, M. Minakata, and S. Kawakami, "Low loss integrated optical Y-branch," *J. Lightwave Technol.*, vol.7, no.5, pp.753–758, May 1989.

- [8] M.H. Hu, J.Z. Huang, R. Scarmozzino, M. Levy, and R.M. Osgood Jr., "A low-loss and compact waveguide Y-branch using refractive-index tapering," *IEEE Photon. Technol. Lett.*, vol.9, no.2, pp.203-205, Feb. 1997.
- [9] C. Manolatos, S.G. Jhonson, S. Fan, P.R. Villeneuve, H.A. Haus, and J.D. Joannopoulos, "High-density integrated optics," *J. Lightwave Technol.*, vol.17, no.9, pp.1682-1692, Sept. 1999.
- [10] A. Sakai and T. Baba, "FDTD simulation of photonic devices and circuits based on circular and fan-shaped microdisks," *J. Lightwave Technol.*, vol.17, no.8, pp.1493-1499, Aug. 1999.
- [11] T. Baba, A. Motegi, T. Iwai, N. Fukaya, Y. Watanabe, and A. Sakai, "Light propagation characteristics of straight single line defect waveguides in photonic crystal slabs fabricated into a silicon-on-insulator substrate," *IEEE J. Select. Topics Quantum Electron.* (2002, to be published).



Atsushi Sakai was born in Saitama Prefecture, Japan, on September 4, 1970. He received the B.E. and M.E. degrees from the Division of Electrical and Computer Engineering, Yokohama National University, Japan, in 1997 and 1999, respectively, and is currently working toward the Ph.D. degree at Yokohama National University, conducting the research focused on micro-photonic devices and circuits by high refractive index difference.

ence.



Tatsuhiko Fukazawa was born in Iwate Prefecture, Japan, on October 23, 1977. He is currently working toward the B.E. degree at Yokohama National University, conducting the research focused on design and fabrication of micro-photonic devices based on SOI substrate.



Toshihiko Baba was born in Nagano Prefecture, Japan, on November 12, 1962. He received the B.E., M.E., and Ph.D. degrees from the Division of Electrical and Computer Engineering, Yokohama National University, Japan, in 1985, 1987, and 1990, respectively. During Ph.D. work, he had been engaged in antiresonant reflecting optical waveguides (ARROW's) and integrated lightwave circuits. From 1990, he has joined the Precision and Intelligence Laboratory, Tokyo Institute of Technology, as a research associate, and started the research on vertical cavity surface emitting lasers (VCSEL's). In 1991, he reported the first calculation of spontaneous emission factor in VCSEL's. In 1993, he achieved the first RT CW operation of a long wavelength VCSEL. In 1994, he became an associate professor at Yokohama National University. He had also held a guest associate professor at Tokyo Institute of Technology, from 1994 to 1999. His current interests are microcavity lasers, photonic band crystals, spontaneous emission control, micromechanical optics, nonlinear optics and optical computing. Dr. Baba is a member of the Japan Society of Applied Physics, and the American Institute of Physics. He received the Niwa Memorial Prize in 1991, the Best Paper Award of Microoptic Conference in 1993 and 1999, and the Paper Award and the Academic Encouragement Award from the IEICE in 1994.